

1



2

3

Journal of Geophysical Research: Solid Earth

4

Supporting Information for

5

**Mechanisms of shear band formation in heterogeneous materials under
compression:**

6

7

The role of pre-existing mechanical flaws

8

9

Manaska Mukhopadhyay, Arnab Roy and Nibir Mandal*

10

High Pressure and Temperature Laboratory, Department of Geological Sciences,

11

Jadavpur University, Kolkata 700032, India.

12

13

14

Contents of this file

15

16

S1: Experimental result of homogenous model deformed at low strain rate

17

S2: Strain profile for MS2

18

S3: Geological Field Study

19

S4: Shear Strain profiles from Field Studies

20

21

22

23

S1. Homogeneous model experiments at lower strain rate

24

We performed an additional set of experiments to test the sensitivity of

25

homogenous PS blocks to strain rate in forming shear band structures (Fig S1). The

26

experiments were run at a lower strain rate, $3 \times 10^{-5} \text{ sec}^{-1}$ to $2 \times 10^{-5} \text{ sec}^{-1}$, as compared to

27

those presented in the main text (Fig 2a). This range of strain rates produced sharp and

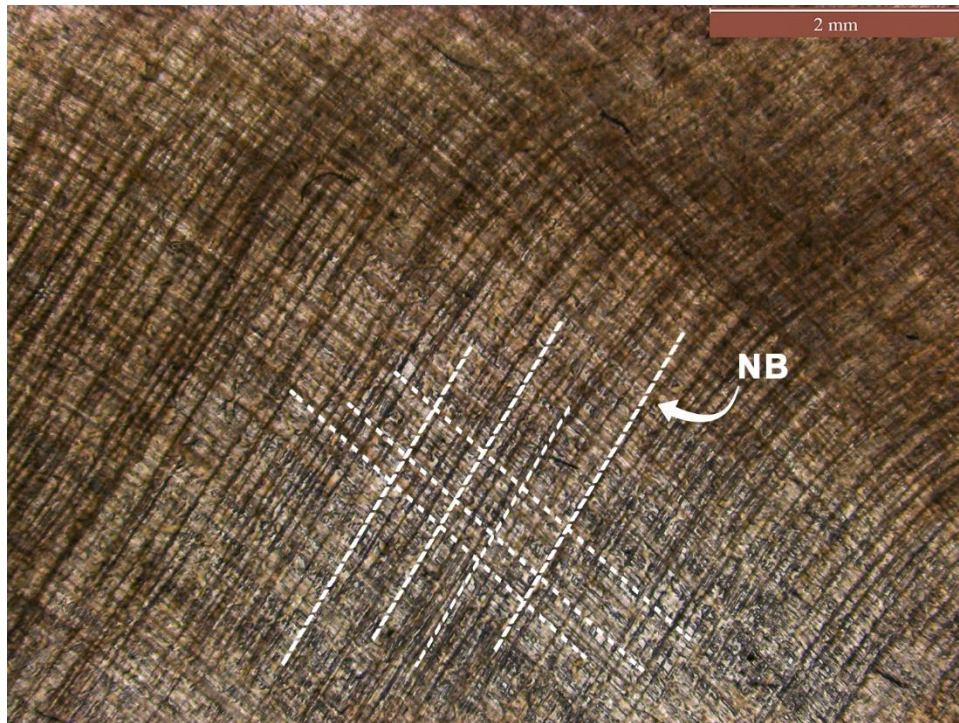
28

narrow bands that are finely spaced and uniformly distributed in the entire model. They

29

typically formed in conjugate sets, symmetrically oriented with respect to the compression

30 direction. The bands multiplied in number with increasing finite strain, as observed in
31 similar experiments at relatively higher rates, and they had no tendency to widen, but grow
32 in length. The PS produced distributed narrow bands in its homogeneous state under the
33 entire range of strain rate conditions used in our laboratory experiments. We thus conclude
34 that uniformly thick bands of homogeneous shear (HBs) in low-strain rate experiments
35 reflect the influence of weak flaws in the model.



36
37 **Figure S1:** Uniform development of closely spaced, conjugate narrow bands (NBs) in
38 homogenous PS models deformed at low strain rate ($\dot{\epsilon} = 2 \times 10^{-5} \text{ sec}^{-1}$). Note that strain
39 rate doesn't have any effect on shear band formation in homogeneous model.

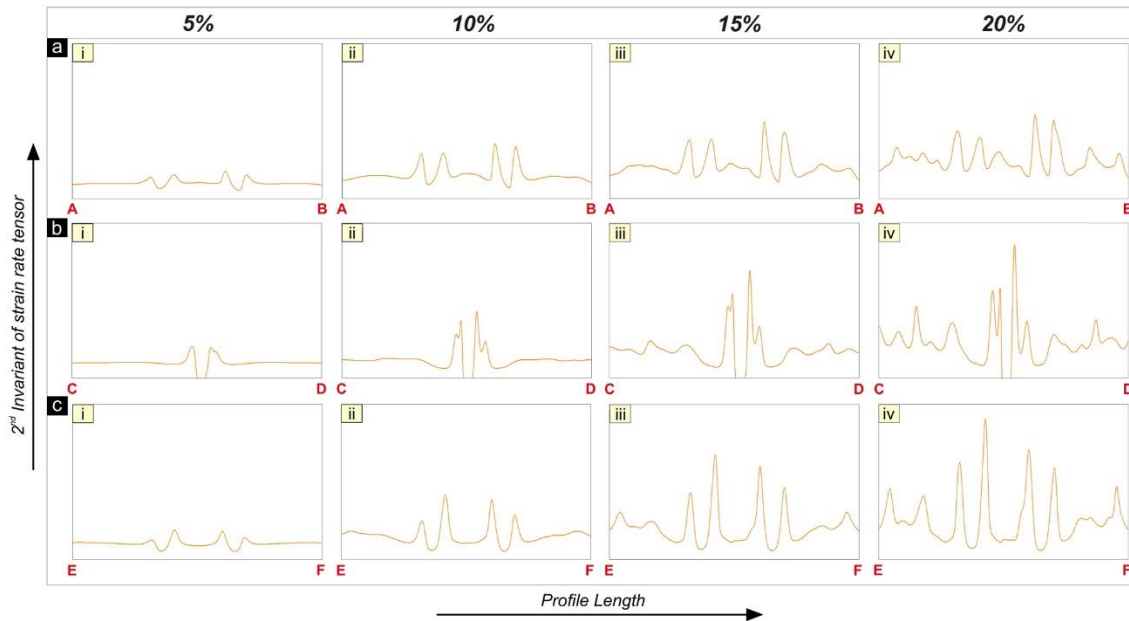
40

41

42 **S2. Across-band strain profiles in numerical models**

43 This section discusses the strain profiles calculated from the numerical simulation
44 MS2 run at relatively high rates (results presented in the main text). The profiles are

45 constructed along the lines AB, CD, EF, as shown in Figure 6 in the main text. They
 46 represent plots of the 2nd invariant of the strain rate tensor (sum of the elastic, viscous and
 47 plastic strain components) as a function of distance in the model. The strain profiles contain
 48 multiple peaks that reveal the composite nature of shear bands, as observed in the PS
 49 experiments at a high strain rate ($3 \times 10^{-5} \text{ sec}^{-1}$).



50

51 **Figure S2:** Across-band strain profiles in MS2 (locations of the profile lines: AB, CD, and
 52 EF, shown in Fig 6). Note that the strain profiles show multiple peaks signifying the
 53 formation of multiple shear bands in the core zone.

54

55

56

57 **S3. Field study of natural shear zones**

58

59

60

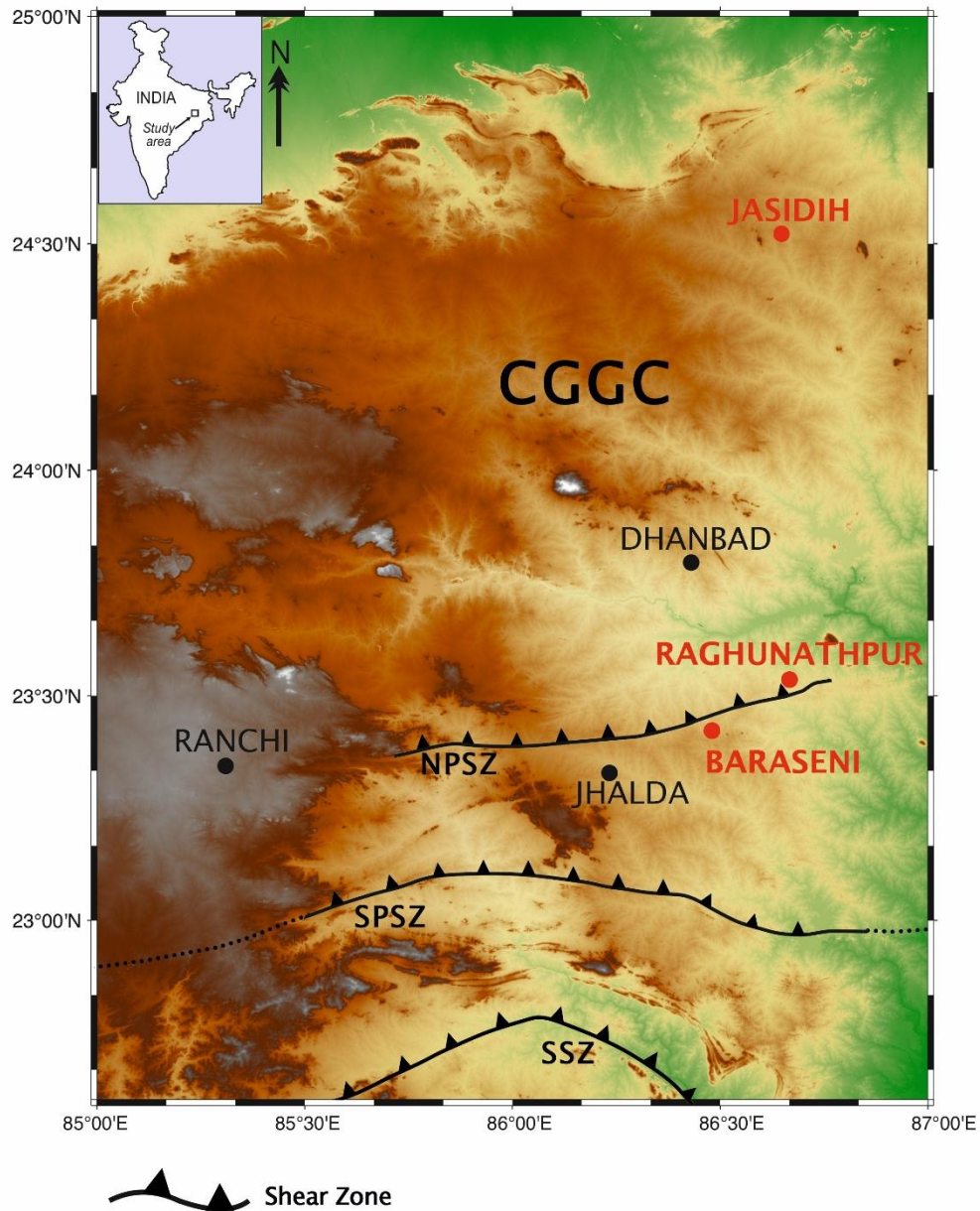
61

We studied a few centimetres to tens of metres long ductile shear zones in the Chotonagpur Granite Gneissic Complex (CGGC), focusing upon regions north of the South Purulia Shear Zone (SPSZ). The shear zones are associated with alkali granite, brecciated quartzite, apatite-magnetite bearing chert, U-Th mineral-bearing pegmatite and mafic-

62 ultramafic rocks. The host rock types include banded, porphyritic and augen granite
63 gneisses, garnet-bearing quartzo-feldspathic gneisses, khondalite, amphibolites and mafic
64 granulites, which generally contain penetrative tectonic foliations of single or multiple
65 generations. The host foliations act as markers, showing sharp deflections across shear
66 bands that allow us to identify the mode of shear localization. In places we could recognize
67 mechanical heterogeneities as nucleating agents of shear zones. For example, high-
68 temperature metamorphic rocks in the Jasidih area show band localization in the vicinity of
69 quartzo-feldspathic aggregates, which possibly represent melt lenses (weak zones)
70 produced by partial melting during the granulite facies metamorphism. This kind of field
71 examples support our experimental interpretation that mechanically weak heterogeneities
72 can be a crucial factor for the formation of isolated shear zones in continua.

73 We chose three prominent locations: 1) Bero Hillocks (23°32'09.5" N, 86°40'01.3"
74 E) near Raghunathpur town, 2) Purulia-Asansol Road transect near Baraseni (23°25'20.9"N
75 86°28'48.8"E), and 3) Jasidih (24° 31' 19.2" N, 86° 38' 51.72" E) (Fig S1). Location 1 is
76 predominantly composed of biotitic granite gneiss, which shows excellent shear band
77 structures with thick strongly shear core, sometimes flanked by excellent drag zones on
78 both sides, while some shows relatively weakly deformed matrix. Lithologically, Location
79 2 is a fine-grained granulite-facies rock, primarily composed of alkali-feldspar, with minor
80 amounts of quartz, mica, garnet and tourmaline. Classically this rock type is also termed
81 as Leptynite and they often show a planar gneissic structure. Location 2 exhibits extensive
82 micro shear band structures with a cross cutting relationship throughout the exposure (Fig
83 8 a). Location 3 is situated near the Jasidih area, which lies in the northernmost part of
84 CGGC. Lithologically, this area is predominantly of migmatitic felsic orthogneiss origin,

85 with random enclaves of meta-sedimentary and meta-mafic rocks. We found excellent
86 shear bands occurring in the vicinity of elliptical to semi-elliptical heterogeneous clasts (Fig
87 8b), that can be well correlated with our heterogeneous models (Fig 2 b).
88



89
90 **Figure S3:** A simplified geological map of the East Indian Precambrian craton, showing
91 the locations of the Singhbhum Shear Zone (SSZ), the South Purulia Shear Zone (SPSZ),
92 the North Purulia Shear Zone (NPSZ) and the Chotanagpur Granite Gneiss Complex
93 (CGGC). Field areas are marked by red dots in the map.

94 **S4. Strain profiles from field studies**

95

96 This section presents the strain profiles obtained from strain analyses performed in

97 field outcrops. Strain profiles were obtained by calculating the finite strain (ϵ) across

98 various types of shear zones. Type I shear zones containing narrow shear bands observed

99 in an area near Purulia town, showed a characteristic curve with a high peak showing large

100 ϵ values implying intense shear localisation across the narrow shear bands (Fig 9b-i). Type

101 II shear zones showed gradational shear strain variation from weakly deformed wall to

102 highly sheared core forming a typical bell-shaped curve (Fig 9b-ii). On the contrary, Type

103 III shear zones are characterized by a plateau like strain profile with very narrow

104 gradational zone (Fig 9b-iii). This characteristic shape results due to formation of a very

105 narrow drag zone on both sides of the homogenous core zone.

106

107

108

109

110

111

112

113

114

115

116

117

118

119

120

121

122

123

124

125

126

127
128

Table S1: Numerical Parameters and Their Values

<i>Parameters</i>	<i>Symbol</i>	<i>Natural Values</i>	<i>Numerical Input Values</i>
Model length	L	60 km	6
Model width	W	40 km	4
Model reference strain rate	$\dot{\gamma}_0$	$1.00e^{-15}$	1
Model reference density	ρ	2700 kg m^{-3}	1
Model reference viscosity	η_0	$1e^{20} \text{ Pas}$	1
Initial Cohesion	C_i	20 Mpa	0.08
Cohesion after Softening	C_s	5 Mpa	0.02
Angle of friction	ϕ	$25^\circ - 30^\circ$	$25^\circ - 30^\circ$
Maximum Yield stress	σ_{\max}	1000 Mpa	3.7
Minimum Yield stress	σ_{\min}	10 Mpa	0.04
Elastic shear module	G	$5 \times 10^9 \text{ Pa}$	18.5

129